Developmental Biology 446 (2019) 80–93

Contents lists available at ScienceDirect

Developmental Biology

journal homepage: www.elsevier.com/locate/developmentalbiology

Drosophila Choline transporter non-canonically regulates pupal eclosion and NMJ integrity through a neuronal subset of mushroom body

Runa Hamid[a,*], Nikhil Hajirnis[a], Shikha Kushwaha[b], Sadaf Saleem[a], Vimlesh Kumar[b], Rakesh K. Mishra[a]

[a] CSIR-Centre for Cellular and Molecular Biology (CSIR-CCMB), Uppal Road, Hyderabad, India
[b] Indian Institute of Science Education and Research, Bhopal, India

ARTICLE INFO

Keywords:
Mushroom body
Drosophila
Choline transporter
Eclosion

ABSTRACT

Insect mushroom bodies (MB) have an ensemble of synaptic connections well-studied for their role in experience-dependent learning and several higher cognitive functions. MB requires neurotransmission for an efficient flow of information across synapses with different flexibility to meet the demand of the dynamically changing environment of an insect. Neurotransmitter transporters coordinate appropriate changes for an efficient neurotransmission at the synapse. Till date, there is no transporter reported for any of the previously known neurotransmitters in the intrinsic neurons of MB. In this study, we report a highly enriched expression of Choline Transporter (ChT) in *Drosophila* MB. We demonstrate that knockdown of ChT in a sub-type of MB neurons called α/β core (α/βc) and ϒ neurons leads to eclosion failure, peristaltic defect in larvae, and altered NMJ phenotype. These defects were neither observed on knockdown of proteins of the cholinergic locus in α/βc and ϒ neurons nor by knockdown of ChT in cholinergic neurons. Thus, our study provides insights into non-canonical roles of ChT in MB.

1. Introduction

Acetylcholine (ACh) is essential for higher cognitive functions and in many of the developmental events of CNS. The components of ACh metabolic cycle namely, Choline acetyltransferase (ChAT), vesicular acetylcholine transporter (VAChT), Acetylcholine esterase (AChE) and Choline transporter (ChT) work in synchronization with each other to bring efficient neurotransmission at cholinergic synapses. Timely removal of ACh from synaptic cleft is a key step of synaptic transmission mediated by AChE. For resynthesis of ACh, ChT transports choline into the presynaptic terminal which is produced by the enzymatic action of Acetylcholine esterase (AChE) at the synapse. There are few, but intriguing evidence, that associate ChT with neuromuscular dysfunction, congenital myasthenic syndrome, severe neurodevelopmental delay and brain atrophy (Barwick et al., 2012; Wang et al., 2017). ChT mutants demonstrate motor activity defects in C. *elegans* (Matthies et al., 2006). Alzheimer's disease has also been associated with altered levels of ChT in cholinergic neurons (Bissette et al., 1996; Pascual et al., 1991). The cognitive significance of ChT has also been indicated in rodents performing various tasks (Durkin, 1994; Toumane et al., 1989; Wenk et al., 1984). Although sparse, all the previous studies bring into focus a highly important role of ChT in cholinergic nerve terminals.

Study demonstrates that intrinsic neurons of *Drosophila* mushroom bodies (MB) are principally cholinergic and express ChAT and VAChT (Barnstedt et al., 2016). Single cell transcriptomics of *Drosophila* mid-brain also recently reported the presence of *VAChT* in many KC's and projection neurons suggesting them to be cholinergic (Croset et al., 2018). This contrasts with the previous findings that show components of the cholinergic cycle are absent from MB (Gorczyca and Hall, 1987; Yasuyama et al., 1995). For an efficient cholinergic neurotransmission in these structures, all the components of the cholinergic cycle should be present. This knowledge is still obscure. It remains unclear whether: (a) all the intrinsic cells of MB are cholinergic in nature or (b) different cells represent a different type of neurochemical. A specific subset of MB intrinsic neurons called α/β core (α/β_c) neurons transiently uses Glutamate as a neurotransmitter at the time of eclosion (Sinakevitch et al., 2010). Studies also show the presence of aspartate and taurine in a limited number of intrinsic neurons of MB (Sinakevitch et al., 2001). Glutamate transporter, vGLUT, is absent from core neurons or other intrinsic neurons of MB (Daniels et al., 2008). Transporters for GABA (DvGAT) and monoamines (DvMAT) are also absent in intrinsic neurons of MB (Chang et al., 2006; Fei et al., 2010). Taken together, different studies

* Corresponding author.
E-mail address: runahamid@ccmb.res.in (R. Hamid).

https://doi.org/10.1016/j.ydbio.2018.12.006
Received 6 August 2018; Received in revised form 25 November 2018; Accepted 7 December 2018
Available online 07 December 2018
0012-1606/

describe different neurotransmitter in intrinsic neurons of MB but the transporters for the known neurotransmitters are absent from these cells. *Drosophila* portabella gene has been previously reported as a putative transporter in MB, but no definitive neurotransmitter has been defined for it (Brooks et al., 2011). In the absence of any transporter, it is not clear how neurotransmitter release and consequently different synaptic strengthening is achieved which might underlie cognitive and developmental events in this structure.

Here, we report for the first time, the presence of ChT in MB and demonstrate a distinct localization of endogenous ChT in all the major lobes of MB. Knockdown of ChT specifically in α/β core (α/β_c) and ϒ neurons lead to severe eclosion failure without affecting any gross larval or pupal development. We also report peristalsis defect and altered NMJ phenotype in these animals. All the three phenotypes: eclosion failure, peristaltic defect, and altered NMJ phenotype are rescued to a significant amount by transgenic over-expression of ChT in α/β_c and ϒ neurons. Furthermore, we demonstrate that the function of ChT in α/β_c and ϒ neurons is independent of the cholinergic pathway. Our results suggest that the role of ChT to transport choline for ACh synthesis might not be exclusive, at least in α/β_c and ϒ neurons. Together, our study reveals a new marker for the *Drosophila* MB and suggests its specific role in eclosion and maintenance of NMJ integrity. Defective NMJ due to knockdown of ChT might be the underlying cause of eclosion failure. In view of any transporter being absent in MB, our findings have broad implications in understanding the functioning of the neural circuits in MB - a region that controls animal behavior and higher cognitive functions.

2. Results

2.1. Choline transporter is enriched in Drosophila mushroom body

ChT is a phylogenetically conserved protein. It was first identified in *C.elegans* followed by rat, mouse, humans and other species (Apparsundaram et al., 2001, 2000; O'Regan et al., 2000; Okuda et al., 2000; Wang et al., 2001). It has a high binding affinity for choline (K_m ~ 1–5 μM) in the nervous system (Kuhar and Murrin, 1978; Lockman and Allen, 2002). *Drosophila* genome also has an annotated ChT homolog, *CG7708*. To study the function of ChT in CNS, we generated a polyclonal antibody against the 125 amino acid long C-terminal of ChT protein. Immunostaining of ventral ganglia with pre-immune sera did not show any immunoreactivity whereas affinity purified anti-ChT serum showed predominant immunoreactivity in the neuropil of ventral nerve cord (VNC) of the third instar larval brain (Fig. S1A-F). This suggests an enrichment of the endogenous ChT protein at the neuropilar synapses. We assessed the specificity of this antibody for the endogenous ChT protein. Immunostaining of larval ventral nerve cord of $Elav^{C155}$GAL4 driven *ChT* RNAi (ChT^{RNAi}) showed a significant reduction of ChT immunoreactivity at the central synapses of VNC as compared to control while costaining with anti-ChAT showed no reduction in immunoreactivity of ChAT protein (Fig. S1G-L). In addition, to determine if the ChT is localized at cholinergic synapses, we assessed colocalization of ChT protein with canonical proteins of the cholinergic cycle, ChAT, and VAChT of the cholinergic locus. By immunostaining of 3rd instar larval VNC, we observed an extensive colocalization of ChT with both ChAT and VAChT in the neuropilar areas (Fig. S2A-F). ChT also colocalizes with ChAT in other cholinergic synaptic rich regions of the brain like Blowig nerve (Fig. S2G-I) and antennal lobes (AL) (Fig. S2J-L). Together, these data show that ChT antibody specifically recognizes endogenous ChT protein at cholinergic synapses of VNC.

In *Drosophila* central brain, we observed that ChT staining was pronounced at the neuropil of the larval central brain and sub-oesophageal ganglia (SOG). It colocalizes extensively with ChAT (Fig. 1A). Strikingly, we observed expression of ChT but not ChAT in the MB of the larval brain (Fig. 1A, A'). This pattern of expression was maintained post-metamorphosis in the adult brain as well (Fig. 1B, B'). During development of the adult brain, the first lobe of MB formed is the ϒ lobe which grows until mid-third instar larval stage. The next is, α'/β' which continues to form till puparium formation. Lastly, α/β lobes are formed from the puparium stage until adult eclosion (Lee et al., 1999). Immunostaining with anti-Disc large (anti-Dlg) and costaining with anti-ChT showed an immense localization of ChT in all the three lobes as well as in spur region of MB (Fig. 1C, D, E, E'). Altogether, these data suggest that ChT is explicitly expressed in all the lobes of *Drosophila* MB. Given the importance of MB in insect behavior, the ubiquitous expression of ChT in MB is intriguing, indicating ChT to be a critical protein for MB physiology and functioning.

2.2. ChT has a vital function in the Drosophila nervous system

Our immunostaining analysis showed that ChT is present ubiquitously throughout the brain. To gain insight into its functional significance in *Drosophila* brain, we used RNAi transgene of *ChT* (ChT^{RNAi}) to cause a reduction in the expression of *ChT* mRNA levels. We expressed ChT^{RNAi} using the pan-neuronal driver, *nSyb*GAL4 (Fig. 2B-D). The expression pattern of this driver in MB was tested with mCD8GFP and co-stained with anti-ChT. The *nSyb*GAL4 expressed mCD8GFP in all the lobes of MB (Fig. 2A). Depletion of ChT in all the neurons showed a drastic reduction in pupation (embryo developed to pupae) as compared to their genetic controls (Fig. 2B-E and Table 1). Likewise, knock down of ChT with another pan-neuronal driver, $Elav^{C155}$ also resulted in reduction in pupation (Fig. 2E and Table 1). Both the pan-neuronal drivers caused the majority of the embryo to not develop to larvae and the embryos which hatched to larvae showed severe motility defect on knock down of ChT in the neurons (Video 1) as compared to their genetic control (Video 2). Very fewer larvae from this progeny progressed to pupae (Table 1). However, majority of progeny that progressed to pupae emerged as adults (Table 2). To establish, if the phenotype observed due to knock down of ChT is neuron-specific only, we used pan-glial driver *repoGAL4*. Using this driver mCD8GFP was expressed and the brains were co-immunostained with anti-ChT for the expression pattern. We observed that glial cells surround the MB and surprisingly, ChT was also localized in glial cells (Fig. 2F-G). Knock down of ChT by ChT^{RNAi} using *repoGAL4* led to a drastic eclosion failure (Fig. 2H and Table 2). Interestingly, knock down of ChAT by $ChAT^{RNAi}$ in glial cells did not show any eclosion failure (Fig. 2H). We also attempted to rescue the eclosion failure phenotype by transgenic over-expression of ChT in neurons and glial cells using these drivers but could not get significant rescue (data not shown). This could probably be due to higher expression of RNAi as compared to the *ChT* transgene by pan-neuronal and pan-glial drivers that masked the effect of *ChT* transgene. Whether ChT plays any role in the functional interaction between glia and neuron is not known and warrants future investigation. However, taken together these observations suggest an essential function of ChT in development and functioning of the *Drosophila* nervous system.

Supplementary material related to this article can be found online at doi:10.1016/j.ydbio.2018.12.006.

2.3. ChT function in α/β core and ϒ neurons of the mushroom body is required for eclosion

To investigate the functional relevance of ChT in MB, we knocked down ChT with ChT^{RNAi}, using GAL4 drivers specific for expression in

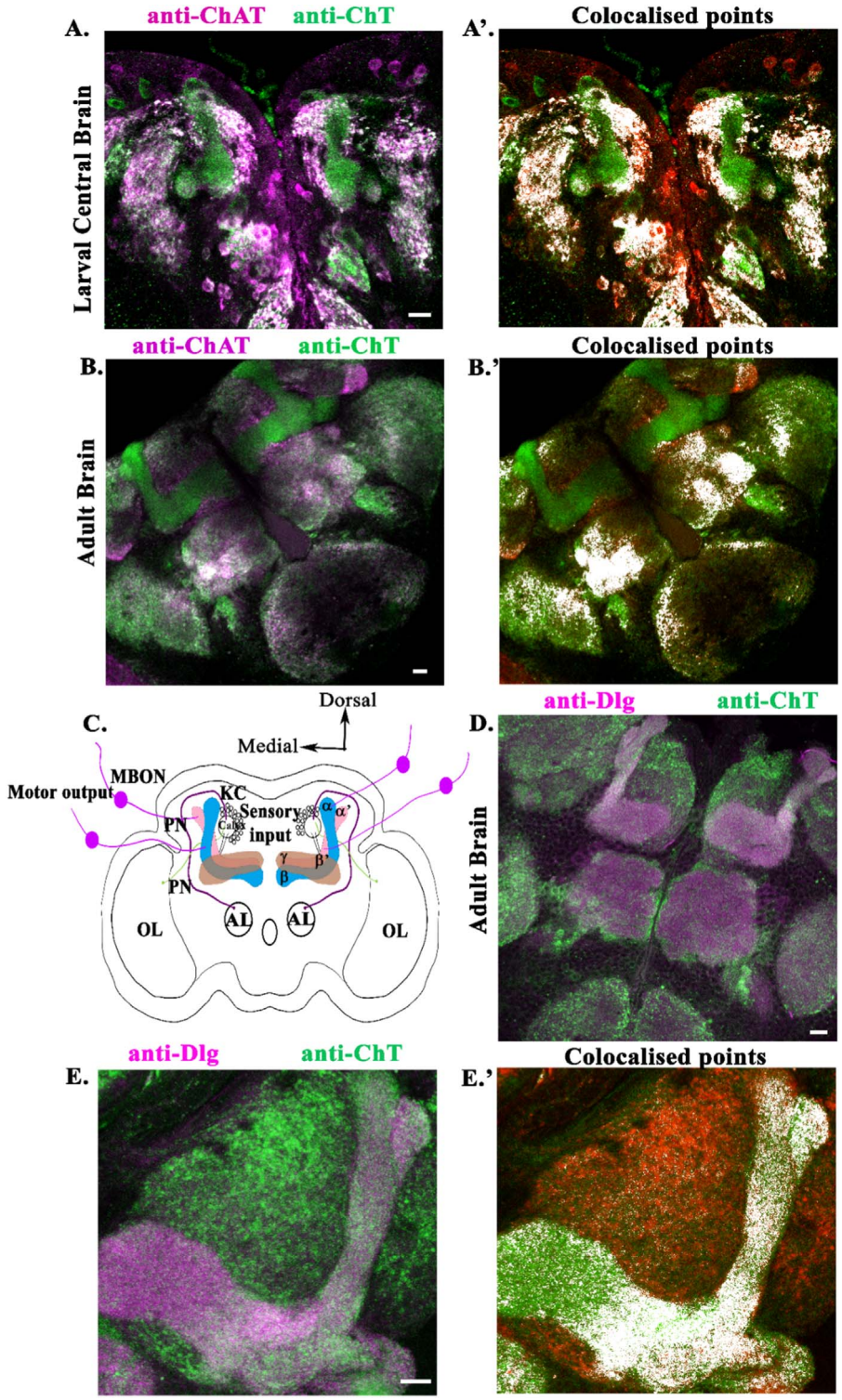

Fig. 1. Ch*T is expressed in MB of larval as well as adult Drosophila brain.* (*A*) left panel, shows co-immunostaining of ChT and ChAT in the central brain of 3rd instar larva, colocalized regions are shown as white, (A') right panel represents the same image processed by image J showing the colocalized pixels as white. (*B*) shows co-immunostaining of ChT and ChAT in the dissected adult fly brain (colocalized regions, white). The L-shaped structures are MB. (B') shows colocalized pixels as white. (*C*), schematics of the fly adult brain showing MB and different neural processes in and out of it. MB circuitry is formed by a posterior cluster of about 2200–2500 Kenyon cells (KC) shown here as empty small circles. KC extend their dendritic processes to form calyx. Projection neurons (PN) from different sensory glomeruli project their axons into the MB calyx. Shown here are antennal lobe (AL) and optic lobe (OL) and representative PN coming out from them as magenta and green respectively. Axons of KCs form fasciculated axonal tract called peduncle which branches into lobes, bifurcating dorsally to form α/α' and medially β/β' (shown as pink and blue lobes). A single ϒ lobe which is continuous with heel wraps β' lobe (shown as brown lobe). The MB lobes synapse with dendrites of Mushroom body output neurons (MBON) which provide the motor input and is the only output of MB (purple solid circle). (*D*) shows the co-immunostaining of Dlg and ChT protein in the adult *Drosophila* brain. (E) shows a digitally zoomed image of Dlg and ChT co-immunostained single MB of the adult brain (left panel) and processed colocalized image (E'). All immunostained images are pseudocolored z-stack confocal images which are representative of 5–7 brains. Scale bar, 50 μm.

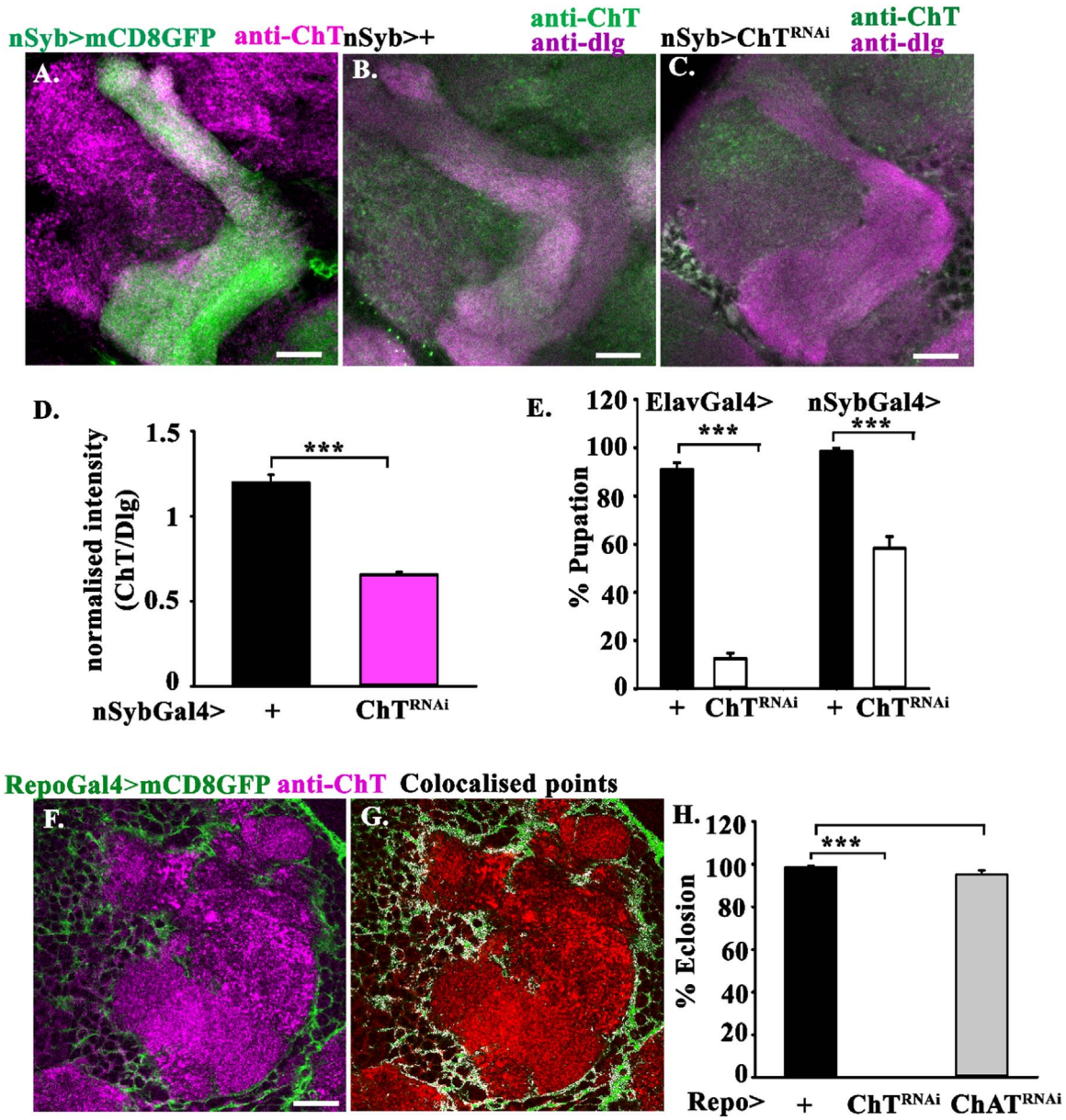

Fig. 2. ***ChT has a vital functional role in both neuronal and glial cell of Drosophila nervous system.*** (A) Shows mCD8GFP expression in all the lobes of MB driven by pan-neuronal, *nSyb*GAL4 (green) and co-stained by anti-ChT (magenta). (B-C) shows knock down of ChT with ChT^{RNAi} driven by *nSyb*GAL4 (nSyb > ChT^{RNAi}) as compared to control (nSyb > +), anti-ChT (green) and coimmunostained with anti-Dlg (magenta), (D) intensity quantification of anti-ChT fluorescence signal normalized to anti-Dlg signal. (E), shows a drastic reduction of percent pupation when ChT was knocked down with pan-neuronal drivers, *nSyb*GAL4 and *Elav*Gal4, as compared to their genetic control (+, drivers crossed with W^{1118}). (F) shows mCD8GFP driven by *repo*GAL4 and (G) shows colocalized points as white while (H) shows eclosion failure as percent eclosion when ChT was knocked down by *repo*GAL4 (*repo*GAL4 > ChT^{RNAi}) as compared to their genetic controls (*repo*GAL4 > +). All images are z-stack pseudocolored representative of 3–5 adult brains. Error bars represent mean ± SEM, * ** represent $p < 0.001$. Statistical analysis is based on one-way ANOVA for pairwise comparison. Scale bar, 50 μm.

different lobes of MB (Aso et al., 2009). The expression pattern of the driver lines was checked by driving expression of mCD8GFP with GAL4 and immunostaining of adult brain with anti-ChT. *201Y*GAL4 showed specific expression in densely packed fibers of α/βc in the center and ϒ lobe (Fig. 3A). Knockdown of ChT in these neurons showed eclosion failure in more than 90% of progeny as compared to the control (Fig. 3B-C and Table 2). The co-staining with anti-ChT and anti-Dlg showed that the anatomy of MB is intact and there is no apparent developmental defect in the overall morphology of the brain due to knock down of ChT (Fig. 3B). We found that *201Y*GAL4 > ChT^{RNAi} flies develop normally throughout the larval and pupal stages (Fig. 3D). However, from these observations, we cannot rule out the possibility of any developmental defect in the establishment of neural circuits, caused due to the reduction of ChT. Indeed, the flies are alive till more than P14 stage (Video 3). Some of the flies were also unable to push themselves out of the pupal case consequently leading to the death of the flies (Video 4). 10% flies escape, display severe flight and motor defects and die within a day or two (Fig. 3C and Table 2). The escapies also show abnormal abdominal melanization and wing expansion failure (data not shown). To confirm if the eclosion failure is due to knock down of ChT in α/βc neurons, the fly was removed from the pupal case and brain was dissected out. Immunostaining of dissected adult brain of *201Y*GAL4 > ChT^{RNAi}, with anti-ChT, showed significant reduction of ChT intensity normalized to the ChT intensity in the neuropilar areas outside MB (Control 1.02 ± 0.09, N = 12; *201Y*GAL4 > ChT^{RNAi} 0.48 ± 0.05, N = 12; Fig. 3E and G). Transgenic overexpression of UAS-*ChT* in MB by *201Y*GAL4 significantly restored ChT levels in MB (*201Y*GAL4/ChT^{RNAi};UAS-ChT, 0.88 ± 0.05, N = 18, Fig. 3F,

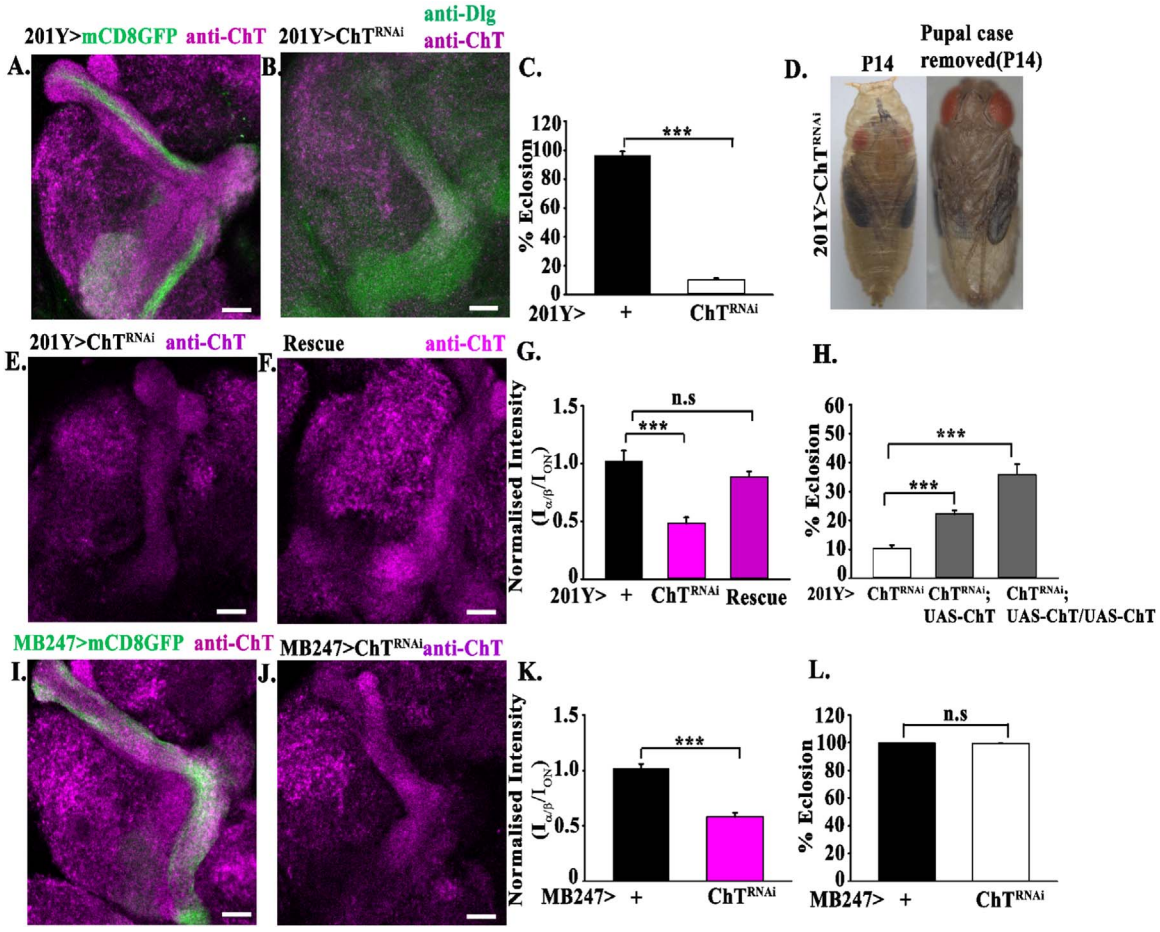

Fig. 3. ***Downregulation of ChT in α/βc neurons lead to eclosion failure which is rescued by transgenic overexpression of ChT.*** (A) Shows mCD8GFP driven by 201YGAL4, marks α/βc neurons and ϒ lobe (green) and co-stained by anti-ChT (magenta) in MB lobe. (B) knockdown of ChT by ChT^{RNAi} is driven by 201YGAL4 and coimmunostained with anti-ChT (purple) and anti-Dlg (green). (C) shows percent eclosion failure by knockdown of ChT in 201Y > ChT^{RNAi} as compared to 201Y > +. (D) shows development in P14 staged undissected pupa (left) and fly dissected out from the pupal case (right) of 201Y > ChT^{RNAi} genotype. (E) shows anti-ChT immunostained brain of 201Y > ChT^{RNAi} flies dissected out from the pupal case. (F) shows anti-ChT immunostained brain of 201Y/ ChT^{RNAi};UAS-ChT/UAS-ChT flies rescued by overexpression of *ChT*. (G) Bar graphs showing quantification of E-F, anti-ChT fluorescence signal inside MB α/β lobes ($I_{α/β}$) normalized to ChT signal in neuropilar areas outside MB lobes (I_{ON}) in indicated genotypes. For rescue dissected adult brain from 201Y/ ChT^{RNAi};UAS-ChT/UAS-ChT was analyzed. (H) shows percent eclosion in 201Y/ ChT^{RNAi};UAS-ChT/+ and 201Y/ ChT^{RNAi}; UAS-ChT/UAS-ChT flies as compared to 201Y > ChT^{RNAi} genotypes. (I) shows mCD8GFP (green) driven by MB247GAL4, marks α/βs and α/βp neurons and co-stained by anti-ChT (magenta) in MB lobe. (J) shows anti-ChT immunostained brain of MB247 > ChT^{RNAi} (K) shows anti-ChT fluorescence signal inside MB α/β lobes ($I_{α/β}$) normalized to ChT signal in neuropilar areas outside MB lobes (I_{ON}) and (L) shows percent eclosion in MB247 > ChT^{RNAi} compared to MB247 > +. All images are z-stack pseudocolored representative of 5–7 adult brains. Error bars represent mean ± SEM, *** represent $p < 0.001$. Statistical analysis is based on one-way ANOVA for pairwise comparison. Scale bar, 50 μm.

and G). We also observed rescue of eclosion failure to a significant level by expression of a single copy of UAS-*ChT* transgene and a double copy of UAS-*ChT* transgene (Fig. 3H and Table 2). Since ChT is present ubiquitously in MB, we explored if knockdown of ChT in other lobes of MB also shows similar eclosion failure. We first checked the expression of another GAL4, MB247GAL4, using UASmCD8GFP. The progeny showed strongly labeled α/β surface (α/βs), α/β posterior (α/βp) but a very weak expression in α/βc and ϒ lobe neurons (Fig. 3I). Knockdown of ChT by expression of *UASChT^{RNAi}* in these neurons showed significant reduction of ChT immunoreactivity in the adult brain of MB247GAL4 > ChT^{RNAi} (Control 1.02 ± 0.09, N = 9; MB247/ChT^{RNAi} 0.58 ± 0.04, N = 12, Fig. 3J-K). However, there was no eclosion failure observed (Fig. 3L). Since ChT knockdown in α/βs and α/βp neurons did not show any eclosion defects, we assessed for mobility defects in these flies using climbing assay. Flies are negatively geotactic and have a natural tendency to move against gravity when agitated. We did not find any significant climbing defects due to reduction of ChT in α/βs and α/βp neurons as compared to controls (Fig. S3A). Knocking down of ChT in α'/β' lobe neurons by *C305a*GAL4 also did not show any eclosion failure compared to their genetic controls (Fig. S3B and Table 2).

Supplementary material related to this article can be found online at doi:10.1016/j.ydbio.2018.12.006.

Because, *201Y*GAL4 drives expression in both α/βc as well as in ϒ lobe (Fig. 3A), therefore we used independent GAL4 drivers, NP6024

Table 1
Quantification of hatched embryo that developed into pupae by downregulation of ChT in indicated genotypes.

Genotypes	Total no. embryos	Pupae formed	% Pupation ± SEM
nSybGal4 > +	2709	2658	97.88 ± 1
nSybGal4 > ChT^{RNAi}	1198	705	57.55 ± 5.32
ElavGal4 > +	732	692	93.05 ± 2.1
ElavGal4 > ChT^{RNAi}	629	75	12.37 ± 2.3
NP6024 > +	1689	1666	98.64 ± 0.6
NP6024 > ChT^{RNAi}	1146	1039	89.91 ± 3
NP6024 > ChT^{RNAi}; UAS-ChT	662	591	90.44 ± 2.26
NP1131 > +	1624	1575	96.31 ± 1.7
NP1131 > ChT^{RNAi}	780	564	75.71 ± 4.0
NP1131 > ChT^{RNAi}; UAS-ChT	913	807	88.71 ± 3.5

Table 2
Genotypes and quantification of pupal viability and eclosion by downregulation of ChT in different subsets of Kenyon cells.

Genotypes	Total no. of pupae	Pupae eclosed	% Eclosion ± SEM
201Y > +	1502	1436	96.49 ± 2.76
201Y > ChT^{RNAi}	957	99	10.3 ± 1.15
201Y > ChT^{RNAi}; UAS-ChT	1246	273	22.2 ± 1.3
201Y > UAS-ChT; UAS-ChT: Ch^{TRNAi}	482	160	35.8 ± 3.7
201Y > VAChT^{RNAi}	495	484	97.46 ± 1.09
201Y > ChAT^{RNAi}	711	694	97.92 ± 1
MB247 > +	1558	1555	99.80 ± 0.15
MB247 > ChT^{RNAi}	1374	1370	99.43 ± 0.41
C305a > +	812	764	95.09 ± 2.28
C305a > ChT^{RNAi}	419	407	96.12 ± 1.99
NP1131 > +	1575	1575	100 ± 0.00
NP1131 > ChT^{RNAi}	564	548	97.60 ± 1.02
NP1131 > ChT^{RNAi}; UAS-ChT	807	796	98.63 ± 0.22
NP6024 > +	1666	1665	99.94 ± 0.06
NP6024 > ChT^{RNAi}	1039	973	92.09 ± 1.85
NP6024 > ChT^{RNAi}; UAS-ChT	591	574	97.41 ± 0.65
ChATGal4 > +	2878	2872	99.78 ± 0.09
ChATGal4 > ChT^{RNAi}	1740	1724	99.09 ± 0.28
ElavGal4 > +	692	688	99.4 ± 0.3
ElavGal4 > ChT^{RNAi}	75	58	81 ± 5.10
nSybGal4 > +	2658	2630	98.98 ± 0.04
nSybGal4 > ChT^{RNAi}	705	689	97.62 ± 0.73
RepoGal4 > +	760	749	98.6 ± 0.6
RepoGal4 > ChT^{RNAi}	241	0	0 ± 0
RepoGal4 > ChAT^{RNAi}	583	514	95.1 ± 1.9

and NP1131 to knock down ChT by *ChT^{RNAi}* in α/βc and ϒ lobe respectively. The expression pattern of both the lines was checked by driving mCD8GFP transgene (Fig. 4A and C.) The knock down of ChT in α/βc neurons, as well as ϒ neurons, showed a significant reduction in eclosion compared to its genetic control (Fig. 4B and D and Tables 1 and 2). Although this effect was not as severe as observed with *201YGAL4*. This is very likely either due to the difference in efficacy of knock down by different GAL4 lines or the severity observed by *201YGAL4* is the additive effect of combined knock down in α/βc and ϒ neurons. We also observed a reduction in pupation in both the cases (Fig. 4B and D and Tables 1 and 2). Percent increase in the pupation as well as the eclosion by transgenic over-expression of UAS-*ChT* in *ChT^{RNAi}* background in α/βc and ϒ neurons was also observed (Tables 1 and 2). Taken together these data suggest a specific role of ChT in α/βc and ϒ neurons to regulate eclosion of adult *Drosophila* flies from the pupal case. ChT seems to play, as yet unidentified function in other neurons of MB. These findings also support the idea that ChT may have a differential function in different intrinsic neurons of KC.

2.4. The function of ChT in α/βc and ϒ neurons is independent of the cholinergic pathway

An earlier study using immunolocalization demonstrated that ChAT and VAChT are absent from MB (Gorczyca and Hall, 1987). On the other hand, microarray analysis in another study suggested that ChAT and VAChT are present to comparable amounts both inside and outside of MB lobes (Perrat et al., 2013). The more recent study shows that KC expresses ChAT and VAChT and suggest that the majority of KC are cholinergic (Barnstedt et al., 2016). In the present study, we reinvestigated for the presence of ChAT and VAChT along with ChT by immunostainings. We observed that ChT shows immense immunoreactivity in all the lobes of MB whereas ChAT immunoreactivity is not detectable (Fig. S4). Although, VAChT shows little immunoreactivity but from these experiments, we cannot rule out the possibility if it is due to extrinsic neuropilar area. To clarify if there are any cholinergic innervations in MB, we expressed mCD8GFP using *ChAT*GAL4. The *ChAT*GAL4 driver contains 7.4 kb 5' flanking genomic sequence of *ChAT* gene (Salvaterra and Kitamoto, 2001). This region has been shown to consist of the regulatory information for the most extensive spatial expression of *ChAT* gene (Kitamoto et al., 1992, 1995; Kitamoto and Salvaterra, 1993). We observed very less amount of mCD8-GFP fibers restricted only to peripheral areas of α/β lobe (Fig. 5A). However, there is a possibility that these fibers belong to the extrinsic cholinergic processes and not to MB. Our results also do not rule out any possibility if the cholinergic driver used is missing regulatory sequences to be expressed in MB. Taken together, our results suggest that there are very less number of cholinergic innervations in MB, if at all any.

We also investigated if the eclosion failure observed due to depletion of ChT is dependent on cholinergic metabolic cycle or not, by downregulating ChT in *ChAT*GAL4 > ChT^{RNAi} flies. We observed that eclosion was perfectly normal (Fig. 5B, Table 2). We quantitated the ChT intensity in *ChAT*GAL4 > ChT^{RNAi} adult brain and observed a significant reduction of ChT in outer neuropilar areas (I_{ON}) as compared to ChT intensity inside α/β lobes ($I_{\alpha/\beta}$). The normalized intensity ($I_{\alpha/\beta}$/ I_{ON}) in *ChAT*GAL4 > ChT^{RNAi} was higher than its genetic control *ChAT*GAL4 > + (Control 1.01 ± 0.08, N = 9; *ChAT*GAL4/ChT^{RNAi} 1.89 ± 0.29, N = 9, Fig. 5C-D). To further confirm the non-cholinergic role of ChT in α/βc and ϒ neurons in eclosion, we downregulated VAChT and ChAT with VAChT^{RNAi} and ChAT^{RNAi} respectively in these neurons using *201Y*GAL4 and did not observe any eclosion failure as compared to its genetic control (Fig. 5E-F and Table 2). The RNAi efficiency of ChAT^{RNAi} and VAChT^{RNAi} was confirmed by immunostainings (Fig. S5A-F and G-L, respectively). Taken together, these data strongly suggest that pupal eclosion failure is specifically due to ChT downregulation in α/βc and ϒ neurons. The function of ChT in these neurons is functionally uncoupled from cholinergic locus suggesting them to be non-cholinergic in nature. It also indicates that ChT is present in a much larger number of KCs which might necessarily not be cholinergic.

2.5. ChT function in α/β core and ϒ neurons regulate peristalsis through a cholinergic independent pathway

Eclosion of flies from the pupal case involves coordinated contraction and relaxation of whole body muscles (Kimura and Truman, 1990; Rivlin et al., 2004). This process helps in the forward movement to drive the fly out of the pupal case. To understand the role of ChT in the observed eclosion failure and whether this defect arises due to ChT in neurons, we assessed the peristaltic movement of late 3rd instar *Drosophila* larvae from caudal to rostral side (forward movement) by knock down of ChT by *ChT^{RNAi}* using pan-neuronal drivers, *nSyB* and *Elav*Gal4. We observed a drastic peristaltic defect in the motility of the larvae in both the cases (Fig. 6A) suggesting the function of ChT in neurons. The *Elav*Gal4 showed much severe defect as compared to *nSyb*Gal4 on ChT knock down which may be attributed to the difference in expression by different promotors.

Since we observed a severe eclosion failure when ChT was knocked down with *201Y*GAL4, therefore we tested if the knock down of ChT also leads to a peristaltic defect in this case. We observed that peristaltic counts were drastically reduced when ChT was depleted in α/βc and ϒ neurons in *201Y*GAL4 > ChT^{RNAi} (47 ± 0.99 counts/min, N = 40) as compared to their genetic controls *201Y*GAL4 > + (61 ± 0.80 contractions/min, N = 40) (Fig. 6B). Transgenic over-expression of *ChT* in these neurons restored the peristaltic decrement (62.41 ± 2.02 counts/min, N = 40) (Fig. 6B). To segregate whether the peristaltic defect was due to α/βc or ϒ neurons, we knocked down ChT in these neurons using NP6024GAL4 and NP1131GAL4 driver lines respectively. Significant peristaltic defects were observed when ChT was knocked down in ϒ neurons (45.5 ± 1.54 counts/min, N = 40) as

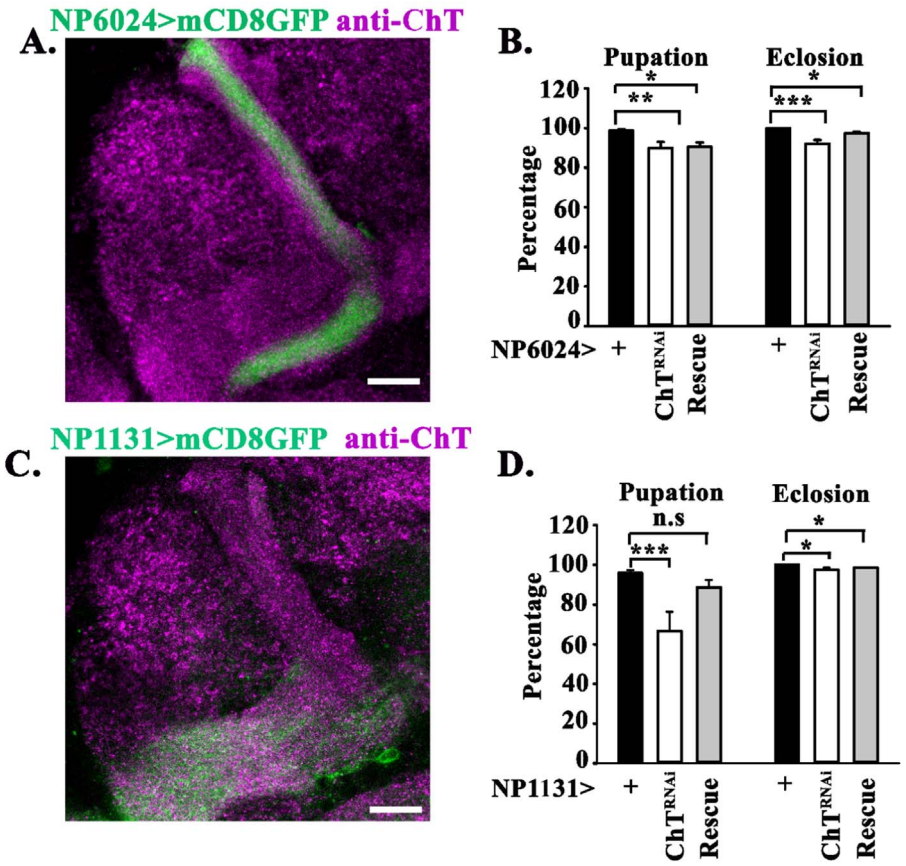

Fig. 4. ***Downregulation of ChT in both α/βc and ϒ neurons lead to a reduction in pupation as well as eclosion*** (A) Shows mCD8GFP driven by NP6024GAL4, marks α/βc neurons (green) and co-stained by anti-ChT (magenta) in MB lobe, (B) bar graphs show percent pupation and eclosion of NP6024GAL4 > +, NP6024GAL4 > ChT^{RNAi} and NP6024GAL4 > ChT^{RNAi};UAS-ChT/+ (Rescue), (C) shows mCD8GFP driven by NP1131GAL4, marks ϒ neurons (green) and co-stained by anti-ChT (magenta) in MB lobe. (D) bar graphs show percent pupation and eclosion of NP1131GAL4 > +, NP1131GAL4 > ChT^{RNAi} and NP1131GAL4 > ChT^{RNAi};UAS-ChT/+ (Rescue). Black boxes represent control, white represent Gal4 driven RNAi, and grey represent rescue genotypes. Images are z-stack pseudocolored representative of 3–5 adult brains. Error bars represent mean ± SEM, *** represent $p < 0.001$, * $p > 0.01$, n.s = non-significant. Statistical analysis is based on one-way ANOVA followed by non-parametric Kruskal-Wallis test where normality test failed. Scale bar, 50 μm.

compared to their genetic control (57.0 ± 1.43 counts/min, N = 40) (Fig. 6C). Similar peristaltic decrement was also observed in α/βc (46.68 ± 2.1 contractions/min, N = 37) as compared to their genetic control (55.65 ± 1.45 contractions/min, N = 48) (Fig. 6D). This implicates role of α/βc and ϒ neurons in peristalsis and larval motility.

To further clarify if the decrease in the peristaltic count is through the cholinergic mode of action and whether this process involves cholinergic proteins, we downregulated ChAT by expression of $ChAT^{RNAi}$ in α/βc and ϒ neurons. We did not observe any significant peristaltic decrease in *201Y*GAL4 > $ChAT^{RNAi}$ larvae (57.46 ± 1.25 counts/min, N = 40) (Fig. 6B). This suggests that the role of ChT is functionally uncoupled from ChAT in MB α/βc and ϒ neurons. Locomotion is one of the important behavior of an animal that largely depends on ACh (Rand, 2007). Therefore, we assessed the effect of ChT downregulation on peristalsis in cholinergic neurons using *ChAT*GAL4. Downregulation of *ChT* in cholinergic neurons reduces peristaltic count (43.46 ± 2.42 counts/min, N = 40) as compared to their genetic control (60 ± 1.82 counts/min, N = 40) (Fig. 6E). This decrement in peristalsis is normalized by transgenic over-expression of *ChT* in cholinergic neurons (61 ± 1.91 contractions/min, N = 40) (Fig. 6E). Intriguingly, like in α/βc neurons, depletion of *ChAT* by $ChAT^{RNAi}$ in cholinergic neurons also does not reduce peristaltic counts (60.13 ± 0.89 counts/min) as compared to their genetic control (Fig. 6E). However, we observed a developmental delay by 3–4 days at 29 °C on knockdown of ChAT in cholinergic neurons as compared to their genetic controls. Taken together, these observations suggest that ChT can have cellular roles independent of the canonical cholinergic pathway. In addition, this data also suggests that the eclosion failure could be due to the defects in contraction and relaxation of body muscles (measured as a peristaltic defect) that arise due to knock down of ChT. The data presented here represents the defects at the late larval stage that arises due to knock down of ChT in MB specific neurons. Whether the eclosion failure is indeed due to defects in contraction and relaxation of body muscles due to knock down of ChT needs further investigation in pharate pupae.

2.6. *ChT function in MB α/βc and ϒ neurons contributes to NMJ maintenance*

Proteins like *Drosophila* neurexins (DNRx), Scribble and RanBPM have been shown to be present in MB and are also associated with NMJ phenotype (Rui et al., 2017; Scantlebury et al., 2010). Therefore, we determined if the locomotor defect caused by downregulation of ChT in α/βc and ϒ neurons could be due to alteration in NMJ morphology. We knocked down *ChT* in expression domain of *201Y* (α/βc and ϒ neurons) and assessed NMJ morphology in 3rd Instar larvae. We found a significant increase in the number of boutons per muscle area at the NMJs of *201Y* > ChT^{RNAi} (1.65 ± 0.06, N = 16) as compared to their genetic control, *201Y* > + (1.32 ± 0.03, N = 16) (Fig. 7A-B and F). There was also an increase in the number of branches in *201Y* > ChT^{RNAi} (10 ± 0.85, N = 16) as compared to the genetic control (5 ± 0.57, N = 16) (Fig. 7A-B and G). This phenotype was significantly rescued by transgenic over-expression of *ChT* in the expression domain of *201Y* neurons (Boutons, 1.34 ± 0.05, N = 10; no. of branches, 8.5 ±

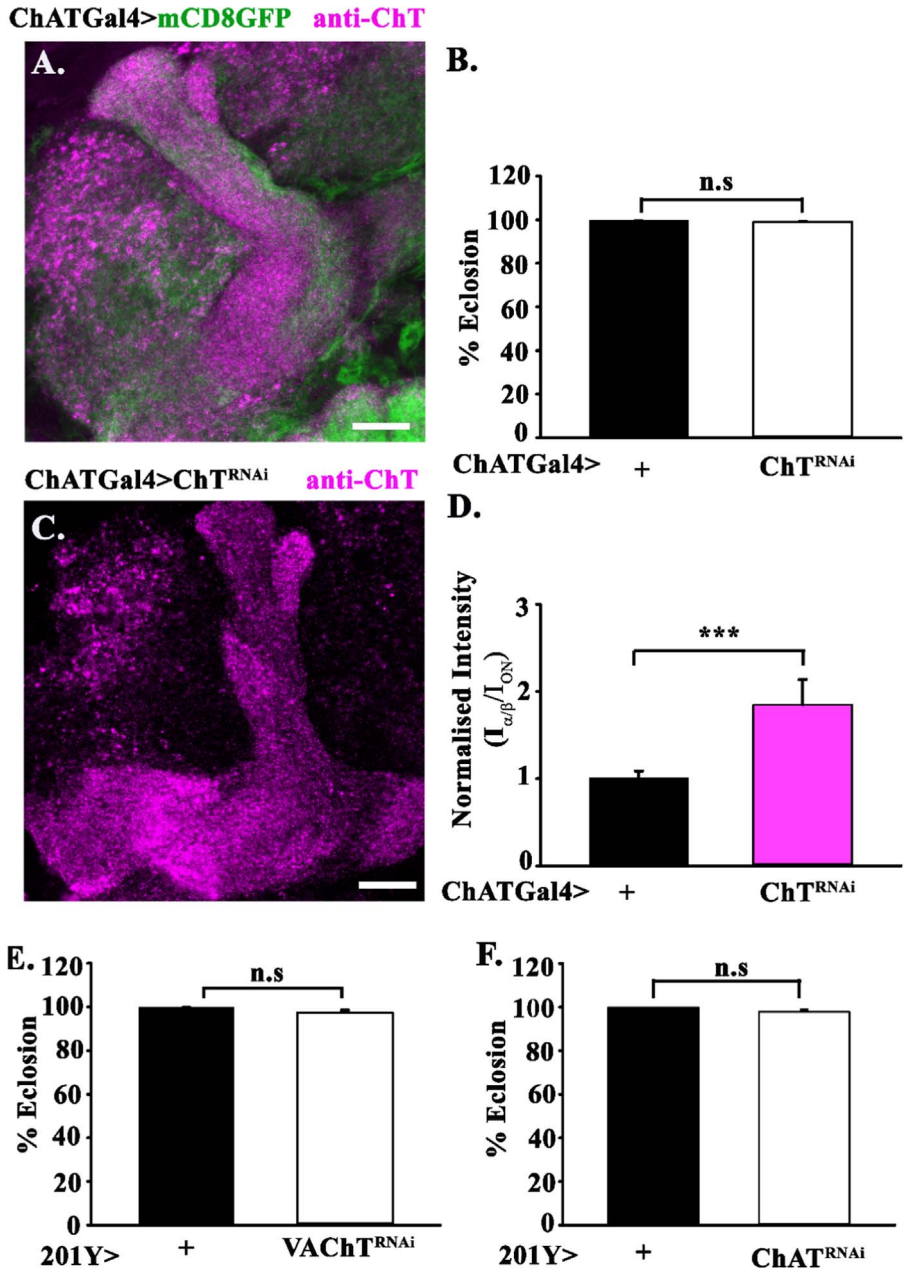

Fig. 5. ***Knockdown of ChT in cholinergic neurons and knock down of cholinergic locus proteins in α/βc neurons do not cause eclosion failure***. (A) Shows mCD8GFP driven by ChATGAL4 that marks cholinergic neuropile (green) and co-stained by anti-ChT (magenta) in the MB lobe. (B) shows percent eclosion failure by knockdown of ChT in ChATGAL4 > ChT^{RNAi} as compared to ChATGAL4 > +. (C) shows the anti-ChT immunostained brain of ChATGAL4 > ChT^{RNAi} flies and (D) are bar graphs showing quantification of anti-ChT fluorescence signal inside MB α/β lobes ($I_{α/β}$) normalized to ChT signal in neuropilar areas outside MB lobes (I_{ON}) in indicated genotypes. (E and F) are percent eclosion by knockdown of ChAT and VAChT in 201Y > $ChAT^{RNAi}$ and 201Y > $VAChT^{RNAi}$ as compared to 201Y > +. All images are a pseudocolored representative image of the 3–5 adult brain. Error bars represent mean ± SEM, *** represent $p < 0.001$. Statistical analysis is based on one-way ANOVA for pairwise comparison. Scale bar, 50 μm.

0.42, N = 11) (Fig. 7C and H-I). Interestingly, downregulation of ChT in cholinergic neurons of *ChAT*GAL4 > ChT^{RNAi} larvae did not show any significant alteration in bouton number (1.09 ± 0.07, N = 10) as well as the number of branches (8.5 ± 0.83, N = 10) as compared to the controls (Boutons, 1.05 ± 0.06; no. of branches, 6.5 ± 0.37) (Fig. 7D-G). We also observed morphological defects in NMJ when ChT was depleted using pan-neuronal, *nSyb*GAL4 driver (Fig. 8A-C). Although, the number of boutons did not show significant alteration (Fig. 8J), number of branches were altered when ChT was reduced in neurons (branches: 11.9 ± 0.4, N = 15) as compared to the controls (branches: 10.23 ± 0.65, N = 13) (Fig. 8K). Transgenic overexpression of ChT by *nSyb*GAL4 restored the altered branch numbers (8.73 ± 0.31, N = 11; Fig. 8K). This suggests that ChT has a role in neurons to maintain NMJ morphology and integrity. To further demarcate which KC subtype, α/βc or ϒ neurons lead to altered NMJ morphology on knock down of ChT, we downregulated ChT in both the KC sub-types separately. We observed that knock down of ChT in α/βc neurons with NP6024GAL4 driver significantly altered bouton number as well as branch number (Bouton 1.93 ± 0.05, N = 17; no. of branches 11 ± 0.49, N = 13) as compared to their genetic controls (Bouton 1.48 ± 0.06, N = 12; no. of branches 9.08 ± 0.43, N = 12) (Fig. 8D-F and L-M). The altered phenotype was rescued by transgenic expression of ChT in these neurons (Bouton 1.63 ± 0.12, N = 16; no. of branches 9.6 ± 0.40, N = 14) (Fig. 8F and L-M). We also observed altered bouton and branch number on knock down of ChT in ϒ neurons by NP1131GAL4 (Bouton 1.93 ± 0.05, N = 18; no. of branches 12.2 ± 0.33, N = 16) as compared

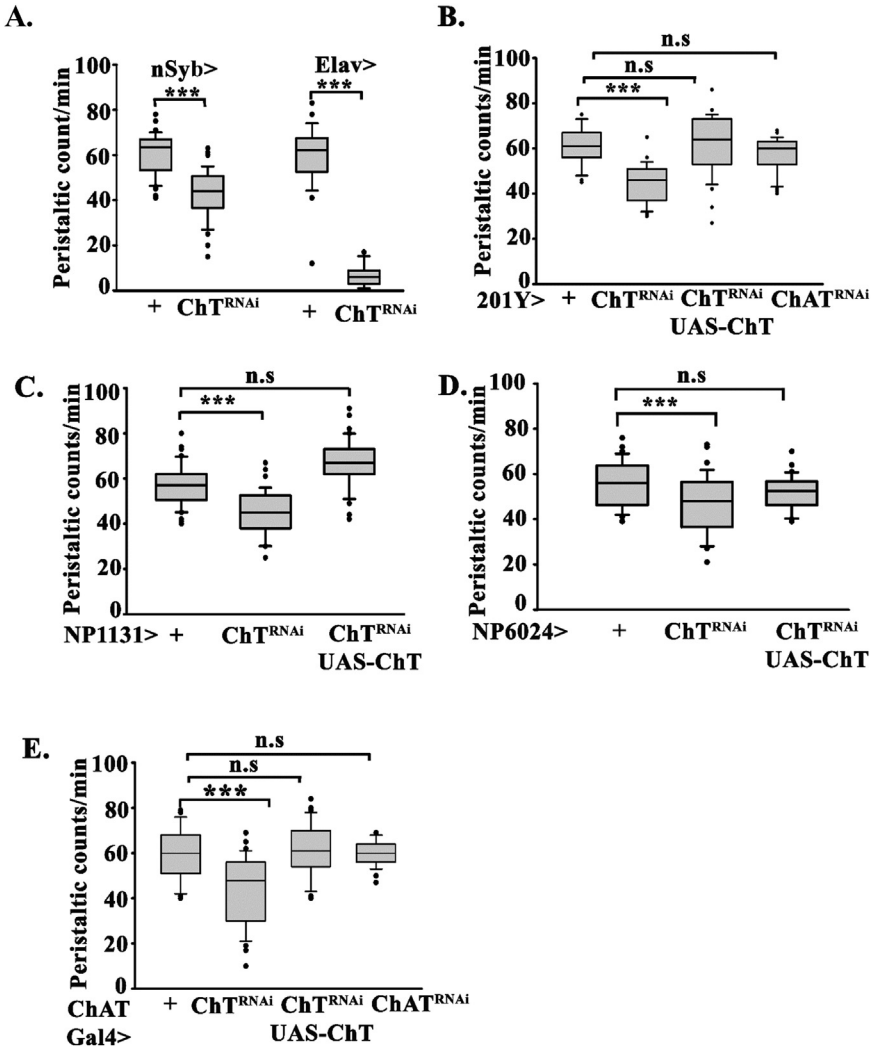

Fig. 6. ***Knockdown of ChT in a subset of MB neurons and cholinergic neurons alter the peristaltic behavior of 3rd instar larvae.*** The figure shows peristalsis quantified as a number of body wall contractions from posterior to anterior end. Data is represented as peristaltic counts per min when ChT was knocked down in the indicated genotypes. (A) with pan-neuronal drivers, *nSyb*GAL4 and *Elav*GAL4, (B) *201Y*GAL4 (expression in α/βc and ϒ neurons) (C) NP1131GAL4 (expression in ϒ neurons), (D) NP6024GAL4 (expression in α/βc neurons), (E) *ChAT*GAL4 (expression in cholinergic neurons). For control driver lines were crossed with W1118 (+) and for rescue driver lines were crossed with ChT^{RNAi};UAS-ChT. Distribution of data is shown as a box plot (N = 35–45) for each genotype. The box plot show box boundaries as 25% and 75% quartiles and median as the center line. 10% and 90% quartiles are shown as whiskers. *** represent $p < 0.001$ and n.s represent non-significance. Statistical analysis is based on one-way ANOVA for pairwise comparison. Kruskal Wallis one-way analysis on variance on ranks was done where the normality test fails.

to their genetic controls (Bouton 1.76 ± 0.05, N = 13; no. of branches 10.8 ± 0.42, N = 13) (Fig. 8G-I and N-O). This phenotype was also rescued by transgenic over-expression of ChT in ϒ neurons (Bouton 1.59 ± 0.12, N = 16; no. of branches 8.5 ± 0.68, N = 17) (Fig. 8I and N-O). We saw significant rescue in both peristaltic and NMJ phenotype but not in eclosion by transgenic over-expression of UAS-*ChT* using NP6024 and NP1131 drivers. This difference in rescue of eclosion failure could be attributed to different GAL4 used because we observed significant rescue of this phenotype by expression of UAS-*ChT* with 201Y driver (Fig. 3H). It could also possibly be due to the differences in the threshold for rescue which might be lower for peristalsis and NMJ phenotype observed while higher for eclosion failure phenotype. Based on these observations, we propose that peristaltic count decrement due to ChT knockdown in α/βc and ϒ neurons may be due to improper NMJ functioning that involves a non-cholinergic pathway for its maintenance. Its decrement in cholinergic neurons affecting peristalsis could be through a different mode of action that involves cholinergic pathway. However, the mechanisms by which ChT controls larval peristaltic movement through a pathway that does not requires ChAT in MB α/βc as well as in cholinergic neurons requires further investigation. Together these results further corroborate our observations that ChT function in α/βc neurons is independent of the cholinergic pathway.

3. Discussion

In the present study, we report that ChT is ubiquitously present in MB and its presence in a specific subset of MB neurons called α/βc and ϒ neurons are important for eclosion from pupae, locomotory behavior, and maintenance of NMJ integrity of *D. melanogaster*. Here, we present evidence that the role of ChT in a subset of MB neurons is functionally uncoupled from the cholinergic locus. Together our results suggest that ChT can affect different downstream functional pathways which can be either cholinergic or non-cholinergic. Our findings thus establish a new avenue for ChT study, that, it is merely not an integral protein of the cholinergic cycle but also has other potential biological functions.

Suppression of ChT in neuronal cells lead to a drastic reduction in pupation and larvae exhibit sluggish movement suggesting a neuronal function of *ChT* gene from early development. Suppression of cholinergic transmission is known to cause locomotory defects and paralysis in *Drosophila*, humans, and *C.elegans* (Kitamoto et al., 2000; Ohno

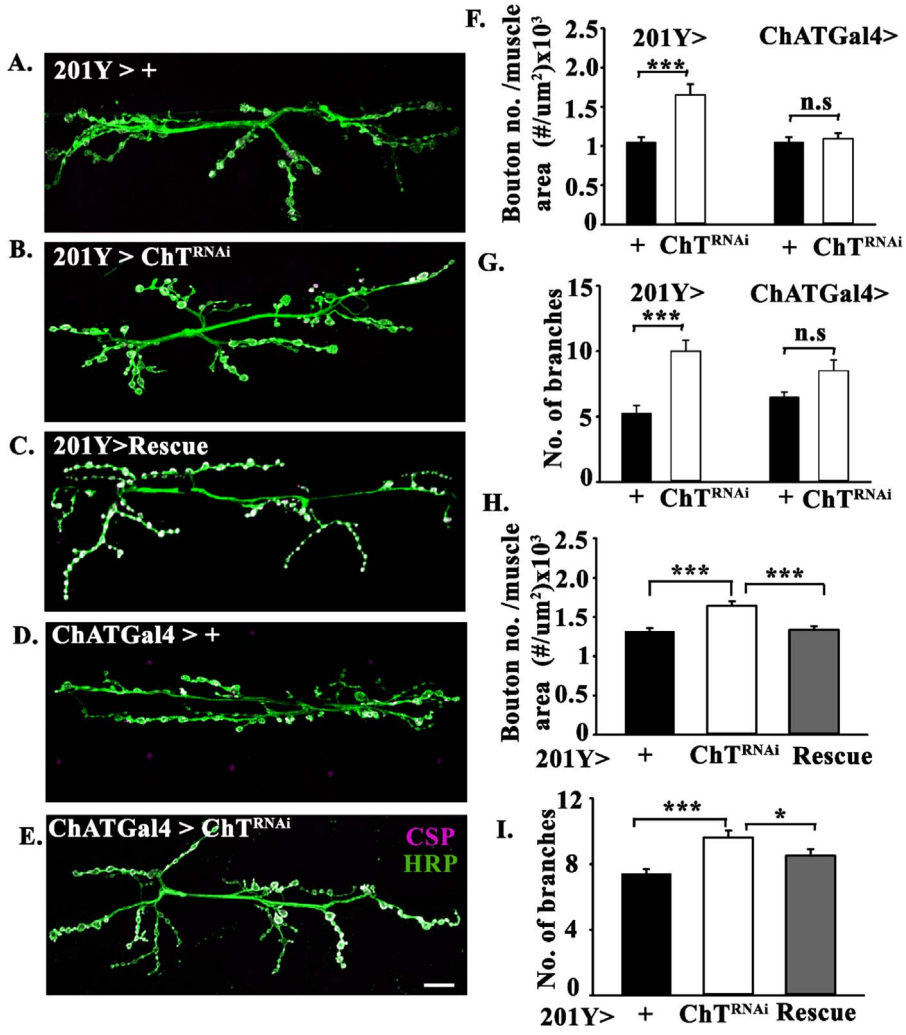

Fig. 7. ***Knockdown of ChT in α/β$_c$ neurons but not in cholinergic neurons alter NMJ phenotype in 3rd instar larvae.*** Representative images of the given genotypes at muscle 6/7 of A2 hemisegment in 3rd instar larva; (A) 201Y > +, (B) 201Y > ChT^{RNAi}, (C) 201Y/ChT^{RNAi};UAS-ChT (Rescue), (D) ChATGal4 > +, (E) ChATGAL4 > ChT^{RNAi}. The NMJs shown were stained with anti-HRP (green) and anti-CSP (magenta). Scale bar in E represents 20 μm. (F-I) Bar graphs showing number of boutons and the total number of branches per muscle area of 6/7 muscle of A2 hemisegment. Error bars represent mean ± SEM; N = 12–17; *** represent $p < 0.001$; * represent $p < 0.05$. Statistical analysis was done using the two-tailed *t*-test and non-parametric Mann-Whitney rank sum test where the normality test failed.

et al., 2001; Rand, 2007). Therefore, the phenotype observed due to knock down of ChT with *ChT^{RNAi}* using pan-neuronal drivers could probably arise from the suppression of cholinergic transmission. We also observed eclosion failure by knock down of ChT in glial cells suggesting ChT function may be required in non-neuronal, glial cells, for viability. Whether the eclosion failure due to knock-down of ChT in glial cells is a cause or consequence of failure seen in neuronal cells need detailed further investigation.

α/βc neurons are the last formed subset of neurons of α/β lobes which are formed between the late pupal stage until adult eclosion (Strausfeld et al., 2003). Our observations that pupal lethality was seen only when ChT was downregulated in α/βc and ϒ but not in α/βp, α/βs neurons of α/β lobe or in α'/β' lobe suggest that ChT plays distinct functional roles in a different subset of MB neurons. We do not observe any defect in the organization of the MB lobes on downregulation of ChT suggesting that it does not have a role in the organization of axonal fibers in these lobes. It is worth mentioning here that ChT knock out mice also showed neonatal lethality while the gross organ development and morphology of the pups were normal (Ferguson et al., 2004). This is closely similar to our observations of eclosion failure and consequent pupal lethality in *Drosophila* due to knock down of ChT. In *Drosophila*, the hydroxyurea treatment to the newly hatched larvae (8–12 h AH) chemically ablates the four neuroblasts that give rise to KC of MB. The flies arising from this treatment have remaining KC of embryonic origin only (de Belle and Heisenberg, 1994; Lovick and Hartenstein, 2015; Prokop and Technau, 1994). In this scenario, flies can normally eclose. The fact that we observed eclosion failure with *201Y*Gal4 may likely be due to the knock down of ChT in progenitor KC that differentiate during the embryonic stage. Indeed, *201Y*GAL4 expression pattern previously showed that many KC survives hydroxy urea treatment (Armstrong et al., 1998). A slight shift of HU treatment from 8 to 12 h to 36–40 h after larval hatching has been reported to cause absence of secondary lineages in larva affecting mostly α/β and α'/β' lobes. The shift in treatment timing also leads to decrease in eclosion (Lovick and Hartenstein, 2015). The loss of mobility and reflex action in such animals has been mentioned in this report too (Lovick and Hartenstein, 2015). This further supports our observations that MB are indispensable for eclosion and mobility and ChT seems to play a role in this process. Another possible cause of eclosion failure may be the altered NMJs that are observed due to knock down of ChT. The underlying mechanism of how ChT in MB neurons affects NMJ morphology is currently unclear. However, like ChT, several other proteins, namely; *Drosophila* Neurexins, Scribble, adaptor protein DRK, and Wallenda have also been reported to have localization in MB and play a role in maintaining structural plasticity at NMJs via different signaling cascades (Moressis et al., 2009; Rui et al., 2017;

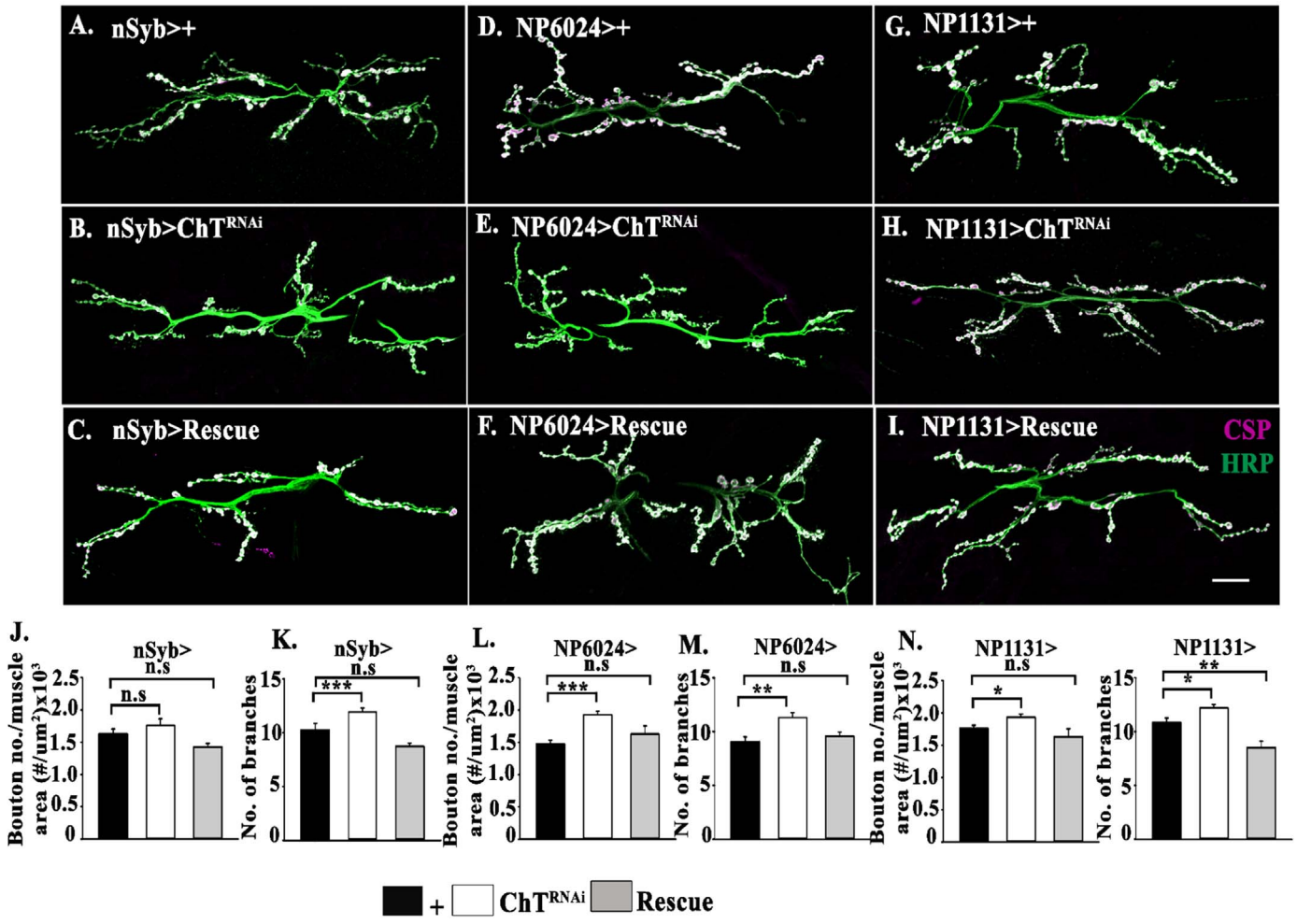

Fig. 8. ***Knockdown of ChT in α/β$_c$ and ϒ neurons alter NMJ phenotype in 3rd instar larvae***. Representative images of the mentioned genotypes at muscle 6/7of A2 hemi-segment in 3rd instar larva; (A) nsybGal4 > +, (B) nsybGal4 > ChT^{RNAi}, (C) nsybGal4 > ChT^{RNAi}; UAS-ChT (Rescue), (D) NP6024 > +, (E) NP6024 > ChT^{RNAi}, (F) NP6024Gal4 > ChT^{RNAi};UAS-ChT/+ (Rescue), (G) NP1131 > +, (H) NP1131 > ChT^{RNAi}, (I) NP1131 > ChT^{RNAi}; UAS-ChT/+ (Rescue). The NMJs shown were co-immunolabeled with anti-HRP (green) and anti-CSP (magenta). Scale bar in I represents 20 μm. (J-O) Bar graphs showing number of boutons per muscle area and the total number of branches. Error bars represent mean ± SEM; N = 12–17; * ** represent p < 0.001; * represent p < 0.05. Statistical analysis was done using the two-tailed *t*-test and non-parametric Mann-Whitney rank sum test where the normality test failed.

Shin and DiAntonio, 2011). Previous reports also describe that MB physiology regulates locomotor activity rhythms in *Drosophila* (Gorostiza et al., 2014; Mabuchi et al., 2016). Future studies are required to elucidate the potential downstream circuit that links the role of ChT in MB physiology and MB motor output.

For an efficient cholinergic neurotransmission, all the components of the ACh metabolic cycle should be present at the synaptic junctions. While there is a predominant expression of ChT in MB, our immunostaining analysis shows that ChAT and VAChT are either absent or present in a negligible amount in MB which is undetectable at endogenous levels with the used antibodies. In the current study, we provide multiple evidences that support non-canonical functions of ChT in α/βc and ϒ neurons: the downregulation of ChT but not ChAT or VAChT in α/βc and ϒ neurons of MB (driven by *201Y*GAL4) cause eclosion failure suggesting that ChT regulates eclosion through a pathway that is functionally uncoupled from the cholinergic locus. Vice-versa, ChT knockdown in cholinergic neurons does not produce eclosion failure. These observations corroborate the idea that ChT can have a non-canonical functional role at least in α/βc and ϒ neurons. Our assertion of the non-canonical role of ChT in MB is further supported by our observations that ChT knockdown in α/βc and ϒ neurons leads to altered phenotype at NMJs showing increased boutons and branch number. This phenotype was not observed when ChT was downregulated in cholinergic neurons. Furthermore, we see a reduction of peristaltic count on knockdown of ChT but not by ChAT in α/βc and ϒ neurons. Indeed, in NSC-19 cells expression of cholinergic locus and ChT was reported to be differentially regulated (Brock et al., 2007). In addition, we also observed eclosion failure by ChT knockdown in glial cells but not by ChAT knock down in these cells which further supports the hypothesis that ChT may have a non-canonical role in different cell types. Although we did not detect ChAT and VAChT in MB but our data do not rule out any non-cell autonomous function of ACh affecting α/β lobe functioning.

Alternatively, ChT in MB may regulate different functions through an indirect downstream pathway. Chromatin remodelers like histone acetyltransferase (HAT) and Histone deacetylase (HDAC4) are dependent on the levels of choline (Ward et al., 2013). They also act as regulators of transcription factors like *D-Mef2* in *Drosophila* MB (Fitzsimons et al., 2013; Fogg et al., 2014) and *FOXP3* in mammals (Li and Greene, 2007). *FOXP* is present in MB and has been associated with locomotor defects and memory deficits (DasGupta et al., 2014). Indeed, we observed similar eclosion failure when we knocked down ChT with *Mef2*GAL4 (data not shown). In the context of our observations, it is possible that ChT in α/βc and ϒ neurons is required for the uptake of choline into these neurons, not for ACh synthesis but different regulatory pathway involved in developmental and behavioral processes. This could be the possible reason that we see eclosion failure and locomotory defects due to ChT knockdown but not by reduction of

cholinergic proteins. Thus, we propose that ChT maintains required levels of choline in α/βc and ϒ neurons for different downstream processes other than ACh synthesis.

Our findings have important implication in redefining the biological role of ChT to affect downstream pathway which may not be cholinergic. We speculate that ChT may be present in the cell types that require a high amount of choline and not just cells that synthesize ACh. Thus, we anticipate that the role of ChT is much far-reaching than previously thought. Although neuroanatomy of flies and vertebrates are quite distinct but the proteins of cholinergic signaling pathway are highly conserved. We believe that it will encourage further investigation into the developmental role of ChT as well as the role it plays in learning and memory in both invertebrates and higher organisms.

4. Material and methods

4.1. Drosophila stocks and culture conditions

All *Drosophila* stocks and their crosses were grown on standard cornmeal/agar media supplemented with yeast at 25 °C, under a 12–12 h light-dark cycle. All crosses for RNAi experiments were grown at 29 °C. For all control experiments, GAL4 drivers crossed with W^{1118} (+) were used, unless otherwise mentioned in the experiments. The UASRNAi strains for ChT (101485), VAChT (32848) were obtained from Vienna *Drosophila* RNAi Center (VDRC), Vienna, Austria and for ChAT (25856) was obtained from Bloomington stock center, Bloomington, Indiana. The GAL4 drivers used were *Elav*^{C155}GAL4 (458), *nSyb*Gal4 (51635) *repo*Gal4 (7415), *ChAT*GAL4 (6798), *201Y*GAL4 (4440), MB247GAL4 (50742), *c305a*GAL4 (30829). NP6024 (105080) and NP1131 (103898) were obtained from DGRC, Kyoto stock center, Japan.

4.2. Cloning and generation of anti-ChT polyclonal antibody

cDNA fragment corresponding to the hydrophilic ChT C-terminal domain (Glu-489 to Phe-614) was amplified by PCR using two oligonucleotide primers 5'AAGGATCCATGGAGTCCGGCAAGTTGCCG CCCA3' and 5'AAAAGCTTTCAGAAGGCCGTATTGTCCT 3'. The amplified fragment was inserted into the *Bam*HI/*Hin*dIII site of the pGEX-KG fusion protein expression vector. The fusion protein was purified and the protein domain was later cleaved from the glutathione S-transferase by incubation with thrombin overnight at 10 °C followed by SDS-polyacrylamide gel electrophoresis to assess the extent of cleavage. The cleaved fragment was eluted and used for immunizing rabbits. About 250 μg of protein was used for the first immunization. For each booster doses (6 ×) 100 μg was used (Deshpande laboratories, Bhopal, India). The antibody from serum was later affinity purified before use.

4.3. Generation of UAS-ChT transgenic line

The open reading frame of ChT was amplified from cDNA using a gene-specific forward primer (5'AAGAATTCATGATCAATATCGCTGGC G-3') and reverse primer (5'AAGCGGCCGCTCAGAAGGCCGTATT GTCCT3'). The amplified fragment was cloned between EcoRI and NotI site of the pUASt vector and injected into *Drosophila* embryos for transgenesis.

4.4. Antibodies and immunohistochemistry of larval and adult brain

The primary antibodies used were: rabbit anti-ChT (1:300, this study), mouse anti-ChAT (1:1000, 4B1, DSHB), anti-VAChT (1:200, a gift from Toshihiro Kitamoto, U. Iowa, Iowa City, IA). Conjugated secondary antibodies used were Alexa Fluor-568 (Molecular Probes), Alexa Fluor 647 (Jackson ImmunoResearch).

For immunohistochemistry, third instar larvae were age-matched and dissected in PBS as previously described (Baqri et al., 2006). For the adult brain, flies were anesthetized on ice and brain tissue was dissected out in cold PBS. Subsequently, tissues were fixed with freshly prepared 4% paraformaldehyde for 1.5 h, washed and incubated with primary antibody at 4 °C overnight. Following day, the tissues were incubated with secondary antibodies for 1.5 h at room temperature, washed and finally mounted in vecatashield in between the bridge prepared by double sided tape in order to avoid squashing of tissue directly under the coverslip. All images were collected using Leica SP8 LSCM using oil immersion 63 × /1.4 N.A objective and subsequently processed using Image J 1.50i (NIH, USA). Pupal images were taken using Zeiss Axiocam ERC 5 S mounted on Zeiss Stemi2000 CS stereomicroscope.

For antibody quantification, three rectangular ROI of 50 × 50-pixel size was drawn over the α/β lobe. The mean fluorescence in the three ROI in α/β lobe ($I_{\alpha/\beta}$) was calculated using Image J. The α/β lobe intensity was normalized with respect to mean fluorescence intensity of the three ROI of 50 × 50-pixel size in the neuropilar area outside MB (I_{ON}).

4.5. Estimation of eclosion failure

Crosses were set between 4 and 5 days old males and virgin females in the ratio of 4:8 and left overnight at 29 °C. Following day, the first vial was discarded and flies were subsequently transferred to new ones with fresh media, every 24 h, for the next seven days. For each day the number of total pupae developed and empty pupal cases were counted. Pupal lethality was scored on the basis of percentage eclosion calculated by [(Number of empty pupae/Total number of pupae) X100]. The quantitative and statistical analysis was performed in Sigma Plot ver. 12.5. One-way ANOVA followed by *post-hoc* Tukey test for pairwise comparison was used.

4.6. Peristalsis assay

Peristalsis assay was done manually on 15 cm petridish containing 2% hardened agar. Larvae were washed and kept on the plate for 1 min acclimatization. Subsequently, the peristaltic contractions were counted for 1 min under a dissection microscope. Full posterior to the anterior movement was counted as one contraction. The larvae which did not move were not considered in the analysis. The quantitative and statistical analysis was performed in Sigma Plot ver. 12.5. One-way ANOVA followed by *post-hoc* Tukey test for pairwise comparison was used.

4.7. Climbing assay

To determine the climbing activity of the flies, the assay vial was prepared by vertically joining two empty polystyrene vials with open ends facing each other. The vertical distance was marked at 6 cm above the bottom surface. A group of 10 flies irrespective of the gender was transferred to fresh vials for 24 h. For the assay, flies were transferred into the assay vial and allowed to acclimatize for 30 min. The flies were then gently tapped down to the bottom of the vial and the number of flies that climb above the 6 cm mark was counted. For each vial three trial readings were taken, allowing for 1 min rest in between each trial. A total of 12 groups were assayed for each genotype. The quantitative and statistical analysis was performed in Sigma Plot ver. 12.5. One-way ANOVA followed by *post-hoc* Tukey test for pairwise comparison was used.

4.8. Immunohistochemistry and morphological quantification of NMJs

Third instar larvae were dissected in the calcium-free HL-3 buffer and fixed in 4% paraformaldehyde for 30 min. Subsequently, larvae

were washed with 1X PBS, 0.2% Triton X-100 and blocked in 5% BSA for 1 h. Incubation of larval fillets was done overnight at 4ºC in primary antibody and then with secondary antibodies for one and a half hour at room temperature and mounted in Flourmount G (Southern Biotech). Antibodies used were mouse anti-CSP (ab49- DSHB) in 1:50 and Alexa 488 conjugated anti-HRP in 1:800 (Molecular Probes). Species-specific fluorophore-conjugated secondary antibody used was Alexa 568 in 1:800 dilution.

Morphological quantification of NMJ was performed at muscle 6/7 in the A2 hemisegment. For quantification of different parameters of NMJ, morphology images were captured at 40× objective in Olympus FV3000. Image J (NIH) and cellSens software were used for muscle area and Bouton number. Bouton number was normalized to respective muscle area. A total number of branches were quantified as described earlier (Coyle et al., 2004). Statistical analysis was done by using students *t*-test and non-parametric Mann-Whitney rank sum test where the normality test failed. All data values indicate mean and standard error mean.

Key resources table.

Reagent or resource	Source	Identifier
Antibodies		
Mouse anti-ChAT	DSHB	ChAT4B1
Rabbit anti-VAChT	Gift from Toshihiro Kitamoto	University of Iowa, IA
Mouse Alexa fluor -568	Molecular probes	Cat# A-11004
Rabbit Alexa fluor 647	Jackson immune research	Cat# 711-605-152
Mouse anti- disc large	DSHB	4F3
Mouse anti-CSP	DSHB	Ab-49
Alexa 488 conjugated anti-HRP	Molecular probes	
Rabbit anti-ChT	This study	N/A
Experimental Models: *Drosophila melanogaster*		
UAS-ChT^{RNAi}	VDRC	V101485
UAS-VAChT^{RNAi}	VDRC	V32848
UAS-ChAT^{RNAi}	BDSC	BL25856
Elav^{C155}GAL4	BDSC	BL458
nSybGAL4	BDSC	51,635
*repo*GAL4	BDSC	7415
*ChAT*GAL4	BDSC	BL6798
*201Y*GAL4	BDSC	4440
*MB247*GAL4	BDSC	50,742
C305aGAL4	BDSC	30,829
NP1131	DGRC	103,898
NP6024	DGRC	105,080
UAS-ChT	This study	
Oligonucleotides		
5'AAGGATCCATGGAGTCC GGCAAGTTGCCGCCCA 3'	7708BamH1 489F'	This study
5'AAAAGCTTTCAGAAGGCCG TATTGTCCT 3'	7708HindIII FLR'	This study
5'AAGAATTCATGATCAATAT CGCTGGCG3'	7708FL EcoR1F'	This study
5'AAGCGGCCGCTCAGAAGGC CGTATTGTCCT3'	7708Not1FLR'	This study
Software and Algorithms		
Image J.	NIH	1.52a
cell Sens	Olympus Life science	

Acknowledgements

We acknowledge Department of Science & Technology, Govt. of India for financial support to R.H vide reference no. SR/WOS-A/LS-77/2013 under Women Scientist Scheme-A to carry out this work. We acknowledge the Indian Institute of Science Education and Research, Bhopal (IISER-B) for hosting R.H during the initial tenure of the project. We thank CCMB advanced microscopy and imaging facility. We thank Toshihiro Kitamoto, for providing *anti*-VAChT antibody, Bloomington Drosophila Stock Center (BDSC), Indiana USA and Vienna Drosophila RNAi Centre (VDRC), Austria, Kyoto stock center, Japan for fly stocks. We also thank Sonal N Jaiswal, Divya Tej Sowpati, Krishanu Ray and Manish Jaiswal for many useful comments on the manuscript.

Author's contributions

Conceptualization, Funding acquisition and project administartion: R.H; Data Curation: R.H; Formal analysis: R.H and N.H; Resources: RKM and V.K, writing original draft: R.H; Review and editing: all authors.

Competing interests

The authors declare no competing or financial interest in publishing this paper.

Reagent availability

All the reagents generated and used in the manuscript will be shared with the scientific community.

Appendix A. Supplementary material

Supplementary data associated with this article can be found in the online version at doi:10.1016/j.ydbio.2018.12.006.

References

Apparsundaram, S., Ferguson, S.M., George, A.L., Jr., Blakely, R.D., 2000. Molecular cloning of a human, hemicholinium-3-sensitive choline transporter. Biochem. Biophys. Res. Commun. 276, 862–867.

Apparsundaram, S., Ferguson, S.M., Blakely, R.D., 2001. Molecular cloning and characterization of a murine hemicholinium-3-sensitive choline transporter. Biochem. Soc. Trans. 29, 711–716.

Armstrong, J.D., de Belle, J.S., Wang, Z., Kaiser, K., 1998. Metamorphosis of the mushroom bodies; large-scale rearrangements of the neural substrates for associative learning and memory in Drosophila. Learn Mem. 5, 102–114.

Aso, Y., Grubel, K., Busch, S., Friedrich, A.B., Siwanowicz, I., Tanimoto, H., 2009. The mushroom body of adult Drosophila characterized by GAL4 drivers. J. Neurogenet. 23, 156–172.

Baqri, R., Charan, R., Schimmelpfeng, K., Chavan, S., Ray, K., 2006. Kinesin-2 differentially regulates the anterograde axonal transports of acetylcholinesterase and choline acetyltransferase in Drosophila. J. Neurobiol. 66, 378–392.

Barnstedt, O., Owald, D., Felsenberg, J., Brain, R., Moszynski, J.P., Talbot, C.B., Perrat, P.N., Waddell, S., 2016. Memory-relevant mushroom body output synapses are cholinergic. Neuron 89, 1237–1247.

Barwick, K.E., Wright, J., Al-Turki, S., McEntagart, M.M., Nair, A., Chioza, B., Al-Memar, A., Modarres, H., Reilly, M.M., Dick, K.J., Ruggiero, A.M., Blakely, R.D., Hurles, M.E., Crosby, A.H., 2012. Defective presynaptic choline transport underlies hereditary motor neuropathy. Am. J. Hum. Genet. 91, 1103–1107.

de Belle, J.S., Heisenberg, M., 1994. Associative odor learning in Drosophila abolished by chemical ablation of mushroom bodies. Science 263, 692–695.

Bissette, G., Seidler, F.J., Nemeroff, C.B., Slotkin, T.A., 1996. High affinity choline transporter status in Alzheimer's disease tissue from rapid autopsy. Ann. N.Y. Acad. Sci. 777, 197–204.

Brock, M., Nickel, A.C., Madziar, B., Blusztajn, J.K., Berse, B., 2007. Differential regulation of the high affinity choline transporter and the cholinergic locus by cAMP signaling pathways. Brain Res. 1145, 1–10.

Brooks, E.S., Greer, C.L., Romero-Calderon, R., Serway, C.N., Grygoruk, A., Haimovitz,

J.M., Nguyen, B.T., Najibi, R., Tabone, C.J., de Belle, J.S., Krantz, D.E., 2011. A putative vesicular transporter expressed in Drosophila mushroom bodies that mediates sexual behavior may define a neurotransmitter system. Neuron 72, 316–329.
Chang, H.Y., Grygoruk, A., Brooks, E.S., Ackerson, L.C., Maidment, N.T., Bainton, R.J., Krantz, D.E., 2006. Overexpression of the Drosophila vesicular monoamine transporter increases motor activity and courtship but decreases the behavioral response to cocaine. Mol. Psychiatry 11, 99–113.
Coyle, I.P., Koh, Y.H., Lee, W.C., Slind, J., Fergestad, T., Littleton, J.T., Ganetzky, B., 2004. Nervous wreck, an SH3 adaptor protein that interacts with Wsp, regulates synaptic growth in Drosophila. Neuron 41, 521–534.
Croset, V., Treiber, C.D., Waddell, S., 2018. Cellular diversity in the Drosophila midbrain revealed by single-cell transcriptomics. Elife 7.
Daniels, R.W., Gelfand, M.V., Collins, C.A., DiAntonio, A., 2008. Visualizing glutamatergic cell bodies and synapses in Drosophila larval and adult CNS. J. Comp. Neurol. 508, 131–152.
DasGupta, S., Ferreira, C.H., Miesenbock, G., 2014. FoxP influences the speed and accuracy of a perceptual decision in Drosophila. Science 344, 901–904.
Durkin, T.P., 1994. Spatial working memory over long retention intervals: dependence on sustained cholinergic activation in the septohippocampal or nucleus basalis magnocellularis-cortical pathways? Neuroscience 62, 681–693.
Fei, H., Chow, D.M., Chen, A., Romero-Calderon, R., Ong, W.S., Ackerson, L.C., Maidment, N.T., Simpson, J.H., Frye, M.A., Krantz, D.E., 2010. Mutation of the Drosophila vesicular GABA transporter disrupts visual figure detection. J. Exp. Biol. 213, 1717–1730.
Ferguson, S.M., Bazalakova, M., Savchenko, V., Tapia, J.C., Wright, J., Blakely, R.D., 2004. Lethal impairment of cholinergic neurotransmission in hemicholinium-3-sensitive choline transporter knockout mice. Proc. Natl. Acad. Sci. USA 101, 8762–8767.
Fitzsimons, H.L., Schwartz, S., Given, F.M., Scott, M.J., 2013. The histone deacetylase HDAC4 regulates long-term memory in Drosophila. PLoS One 8.
Fogg, P.C., O'Neill, J.S., Dobrzycki, T., Calvert, S., Lord, E.C., McIntosh, R.L., Elliott, C.J., Sweeney, S.T., Hastings, M.H., Chawla, S., 2014. Class IIa histone deacetylases are conserved regulators of circadian function. J. Biol. Chem. 289, 34341–34348.
Gorczyca, M.G., Hall, J.C., 1987. Immunohistochemical localization of choline acetyltransferase during development and in Chats mutants of Drosophila melanogaster. J. Neurosci. 7, 1361–1369.
Gorostiza, E.A., Depetris-Chauvin, A., Frenkel, L., Pirez, N., Ceriani, M.F., 2014. Circadian pacemaker neurons change synaptic contacts across the day. Curr. Biol. 24, 2161–2167.
Kimura, K.I., Truman, J.W., 1990. Postmetamorphic cell death in the nervous and muscular systems of Drosophila melanogaster. J. Neurosci. 10, (403-401).
Kitamoto, T., Salvaterra, P.M., 1993. Developmental regulatory elements in the 5' flanking DNA of the Drosophila choline acetyltransferase gene. Roux Arch. Dev. Biol. 202, 159–169.
Kitamoto, T., Ikeda, K., Salvaterra, P.M., 1992. Analysis of cis-regulatory elements in the 5' flanking region of the Drosophila melanogaster choline acetyltransferase gene. J. Neurosci. 12, 1628–1639.
Kitamoto, T., Ikeda, K., Salvaterra, P.M., 1995. Regulation of choline acetyltransferase/lacZ fusion gene expression in putative cholinergic neurons of Drosophila melanogaster. J. Neurobiol. 28, 70–81.
Kitamoto, T., Xie, X., Wu, C.F., Salvaterra, P.M., 2000. Isolation and characterization of mutants for the vesicular acetylcholine transporter gene in Drosophila melanogaster. J. Neurobiol. 42, 161–171.
Kuhar, M.J., Murrin, L.C., 1978. Sodium-dependent, high affinity choline uptake. J. Neurochem. 30, 15–21.
Lee, T., Lee, A., Luo, L., 1999. Development of the Drosophila mushroom bodies: sequential generation of three distinct types of neurons from a neuroblast. Development 126, 4065–4076.
Li, B., Greene, M.I., 2007. FOXP3 actively represses transcription by recruiting the HAT/HDAC complex. Cell Cycle 6, 1432–1436.
Lockman, P.R., Allen, D.D., 2002. The transport of choline. Drug Dev. Ind. Pharm. 28, 749–771.
Lovick, J.K., Hartenstein, V., 2015. Hydroxyurea-mediated neuroblast ablation establishes birth dates of secondary lineages and addresses neuronal interactions in the developing Drosophila brain. Dev. Biol. 402, 32–47.
Mabuchi, I., Shimada, N., Sato, S., Ienaga, K., Inami, S., Sakai, T., 2016. Mushroom body signaling is required for locomotor activity rhythms in Drosophila. Neurosci. Res. 111, 25–33.
Matthies, D.S., Fleming, P.A., Wilkes, D.M., Blakely, R.D., 2006. The Caenorhabditis elegans choline transporter CHO-1 sustains acetylcholine synthesis and motor function in an activity-dependent manner. J. Neurosci. 26, 6200–6212.
Moressis, A., Friedrich, A.R., Pavlopoulos, E., Davis, R.L., Skoulakis, E.M., 2009. A dual role for the adaptor protein DRK in Drosophila olfactory learning and memory. J. Neurosci. 29, 2611–2625.
Ohno, K., Tsujino, A., Brengman, J.M., Harper, C.M., Bajzer, Z., Udd, B., Beyring, R., Robb, S., Kirkham, F.J., Engel, A.G., 2001. Choline acetyltransferase mutations cause myasthenic syndrome associated with episodic apnea in humans. Proc. Natl. Acad. Sci. USA 98, 2017–2022.
Okuda, T., Haga, T., Kanai, Y., Endou, H., Ishihara, T., Katsura, I., 2000. Identification and characterization of the high-affinity choline transporter. Nat. Neurosci. 3, 120–125.
O'Regan, S., Traiffort, E., Ruat, M., Cha, N., Compaore, D., Meunier, F.M., 2000. An electric lobe suppressor for a yeast choline transport mutation belongs to a new family of transporter-like proteins. Proc. Natl. Acad. Sci. USA 97, 1835–1840.
Pascual, J., Fontan, A., Zarranz, J.J., Berciano, J., Florez, J., Pazos, A., 1991. High-affinity choline uptake carrier in Alzheimer's disease: implications for the cholinergic hypothesis of dementia. Brain Res. 552, 170–174.
Perrat, P.N., DasGupta, S., Wang, J., Theurkauf, W., Weng, Z., Rosbash, M., Waddell, S., 2013. Transposition-driven genomic heterogeneity in the Drosophila brain. Science 340, 91–95.
Prokop, A., Technau, G.M., 1994. Normal function of the mushroom body defect gene of Drosophila is required for the regulation of the number and proliferation of neuroblasts. Dev. Biol. 161, 321–337.
Rand, J.B., 2007. AcetylcholineWormBook, 1–21.
Rivlin, P.K., St Clair, R.M., Vilinsky, I., Deitcher, D.L., 2004. Morphology and molecular organization of the adult neuromuscular junction of Drosophila. J. Comp. Neurol. 468, 596–613.
Rui, M., Qian, J., Liu, L., Cai, Y., Lv, H., Han, J., Jia, Z., Xie, W., 2017. The neuronal protein Neurexin directly interacts with the Scribble-Pix complex to stimulate F-actin assembly for synaptic vesicle clustering. J. Biol. Chem. 292, 14334–14348.
Salvaterra, P.M., Kitamoto, T., 2001. Drosophila cholinergic neurons and processes visualized with Gal4/UAS-GFP. Brain Res. Gene Exp. Patterns 1, 73–82.
Scantlebury, N., Zhao, X.L., Rodriguez Moncalvo, V.G., Camiletti, A., Zahanova, S., Dineen, A., Xin, J.H., Campos, A.R., 2010. The Drosophila gene RanBPM functions in the mushroom body to regulate larval behavior. PLoS One 5, e10652.
Shin, J.E., DiAntonio, A., 2011. Highwire regulates guidance of sister axons in the Drosophila mushroom body. J. Neurosci. 31, 17689–17700.
Sinakevitch, I., Farris, S.M., Strausfeld, N.J., 2001. Taurine-, aspartate- and glutamate-like immunoreactivity identifies chemically distinct subdivisions of Kenyon cells in the cockroach mushroom body. J. Comp. Neurol. 439, 352–367.
Sinakevitch, I., Grau, Y., Strausfeld, N.J., Birman, S., 2010. Dynamics of glutamatergic signaling in the mushroom body of young adult Drosophila. Neural Dev. 5, 10.
Strausfeld, N.J., Sinakevitch, I., Vilinsky, I., 2003. The mushroom bodies of Drosophila melanogaster: an immunocytological and golgi study of Kenyon cell organization in the calyces and lobes. Microsc. Res. Tech. 62, 151–169.
Toumane, A., Durkin, T., Marighetto, A., Jaffard, R., 1989. The durations of hippocampal and cortical cholinergic activation induced by spatial discrimination testing of mice in an eight-arm radial maze decrease as a function of acquisition. Behav. Neural Biol. 52, 279–284.
Wang, H., Salter, C.G., Refai, O., Hardy, H., Barwick, K.E.S., Akpulat, U., Kvarnung, M., Chioza, B.A., Harlalka, G., Taylan, F., Sejersen, T., Wright, J., Zimmerman, H.H., Karakaya, M., Stuve, B., Weis, J., Schara, U., Russell, M.A., Abdul-Rahman, O.A., Chilton, J., Blakely, R.D., Baple, E.L., Cirak, S., Crosby, A.H., 2017. Choline transporter mutations in severe congenital myasthenic syndrome disrupt transporter localization. Brain 140, 2838–2850.
Wang, Y., Cao, Z., Newkirk, R.F., Ivy, M.T., Townsel, J.G., 2001. Molecular cloning of a cDNA for a putative choline co-transporter from Limulus CNS. Gene 268, 123–131.
Ward, C.S., Eriksson, P., Izquierdo-Garcia, J.L., Brandes, A.H., Ronen, S.M., 2013. HDAC inhibition induces increased choline uptake and elevated phosphocholine levels in MCF7 breast cancer cells. PLoS One 8, e62610.
Wenk, G., Hepler, D., Olton, D., 1984. Behavior alters the uptake of [3H]choline into acetylcholinergic neurons of the nucleus basalis magnocellularis and medial septal area. Behav. Brain Res. 13, 129–138.
Yasuyama, K., Kitamoto, T., Salvaterra, P.M., 1995. Localization of choline acetyltransferase-expressing neurons in the larval visual system of Drosophila melanogaster. Cell Tissue Res. 282, 193–202.